Interface Properties of Perfluorinated Iron Phthalocyanine on Au(111) and Ag(111): The Influence of Iron and the Macrocycle

Axel Belser, Katharina Greulich, Peter Nagel, Michael Merz, Stefan Schuppler, Thomas Chassé, and Heiko Peisert*

ABSTRACT: The molecular orientation and interface properties of Fe(II) hexadecafluoro-phthalocyanine ($FePcF_{16}$) on Ag(111) are investigated by photoexcited electron spectroscopies: X-ray photoemission spectroscopy (XPS), X-ray absorption spectroscopy (XAS), and resonant photoemission (ResPES). The data are compared to those for $FePcF_{16}$ on Au(111). The molecules are oriented predominantly flat, lying on both substrate surfaces; increased tilts are observed for $FePcF_{16}$ on Au(111). On Ag(111), the electronic structure of $FePcF_{16}$ is distinctly altered at the interface, involving both the macrocycle and the central metal atom. An interface state close to the Fermi energy exhibits a clear Fe character.

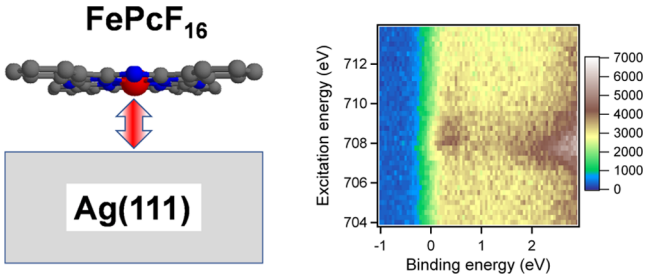

1. INTRODUCTION

Molecules from the family of metal phthalocyanines (MPcs) have been extensively applied in numerous molecular devices. Recently, opto-electronic devices such as light-emitting diodes, field-effect transistors, solar cells, and spintronic devices have become the focus of research.[1−7] In contrast to other MPcs, the electronic structure of iron phthalocyanine (FePc) is very complex, in particular at interfaces.[8−11] Recent studies on $FePcF_{16}$/metal interfaces indicate that the electronic structure of Fe is affected by the fluorination, an essential role played most likely by the versatile arrangement of the molecules in thin films.[12,13]

At many MPc/metal interfaces, stronger interactions including charge transfer were observed. Such an interfacial charge transfer may occur via different interaction channels: the central metal atom and/or the macrocycle of the phthalocyanine molecule. The latter mechanism depends crucially on the relative position of frontier molecular orbitals with respect to the Fermi level of the substrate. Thus, the fluorination of phthalocyanines, significantly changing the ionization potential (IP),[14,15] represents an ideal route for the tuning of interface properties. Moreover, perfluorinated phthalocyanines belong to the earliest-reported, air-stable n-type organic semiconductors.[16−19] Although FePc/metal interfaces have been intensely studied during the past years (e.g., refs 20−26), less is known about the interfaces between the perfluorinated relative ($FePcF_{16}$) and metals.

Here, we study the electronic interface properties and molecular orientation of $FePcF_{16}$ on Ag(111). The more inert $FePcF_{16}$/Au(111) interface serves as a reference system (cf. also ref 27). For the study, we apply photoemission (PES), X-ray absorption spectroscopy (XAS), and resonant photoemission spectroscopy (ResPES).

2. EXPERIMENTAL SECTION

Au(111) and Ag(111) single crystals were cleaned by cycles of argon ion sputtering and annealing. The sputtering was carried out at voltages of 0.8−1.0 kV for typically 30 min at an Ar pressure of 1×10^{-6} mbar; the subsequent annealing was performed for 30 min at temperatures of 770 K (Au(111)) and 800 K (Ag(111)). Substrate temperatures were measured using a pyrometer. $FePcF_{16}$, purchased from SYNTHON Chemicals GmbH & Co. KG, was resublimed and thoroughly degassed in vacuo. The molecules were evaporated at rates of about 1−2 Å/min, determined by a quartz microbalance. The evaporation temperature was about 650 K (measured using a thermocouple), and the substrate was held at room temperature. The indicated film thickness was determined by a comparison of the photoemission intensities of the substrate and related overlayer peaks assuming layer-by-layer growth. Atomic cross sections were taken from ref 28.

XAS, PES, and ResPES measurements were performed at the WERA beamline at the Karlsruhe Research Accelerator (KARA, Karlsruhe, Germany). The energy resolution for XAS and PES was set to 220 and 340 meV at photon energies of

400 and 710 eV, respectively. The degree of polarization for XAS was about 95%. The energy scale of PES was calibrated to reproduce the binding energies (BE) of Au $4f_{7/2}$ and Ag $3d_{5/2}$ (84.0 and 368.2 eV). The absorption was monitored indirectly by measuring the total electron yield (sample current). The X-ray absorption (XA) spectra was normalized to the same step height well above the ionization threshold. For photon energy calibration, the energy of the Ni-L_3 absorption edge of NiO at 853.0 eV was taken as a reference. The peak fitting of XP spectra was performed using the program Unifit,[29] with Voigt profile (convolution of Gaussian and Lorentzian) line shape and a Shirley model background.

3. RESULTS AND DISCUSSION

3.1. Molecular Orientation in Thin Films. The growth of organic molecules can influence intermolecular interactions to a large extent and thus, is a determining factor for the electronic structure of thin films. Moreover, the orientation at interfaces can significantly affect the strength of the interaction between the molecule and the substrate under consideration. Planar transition metal phthalocyanines (TMPcs) often grow in a flat-lying geometry with respect to the substrate surface on single crystalline metal substrates (e.g., refs 25, 30−33). On the other hand, the fluorination may affect the growth mode significantly.[19,34,35]

The molecular orientation of $FePcF_{16}$ on Au(111) and Ag(111) surfaces was studied using polarization-dependent XAS. For planar π-conjugated carbon systems, the molecular orientation can be probed by monitoring the relative intensities of excitations from the occupied C 1s core levels to the unoccupied molecular levels (π^* or σ^*).[36] In a planar conjugated carbon system, the excitation from C 1s to a π^* orbital is maximal for E vertical to the molecular plane (parallel to $2p_z$), whereas the transition to σ^* is maximal for E parallel to the molecular plane and to the chemical bond. For phthalocyanines, besides C 1s-π^*, in a similar manner, also N 1s-π^* excitations can be used for the analysis of the molecular orientation,[30] avoiding the problems of the analysis of C 1s-π^* spectra arising from common carbon contaminations of beamline components.

In Figure 1, we show the N-K edge absorption spectra of thin films of $FePcF_{16}$ on Au(111) and Ag(111) as a function of the incidence angle θ of the p-polarized synchrotron radiation to investigate the orientation of the molecules on the different substrates (see the inset). The region at photon energies below 402 eV belongs to transitions into the π^*-orbitals, and the region above to σ^*-transitions, although we note that weak in-plane polarized transitions appear below 402 eV.[30,37,38]

On both substrates, the spectra show strong out-of-plane π^*-transitions at grazing incidence (10°). At normal incidence (90°), strong in-plane σ^*-transitions can be observed. This suggests that the molecules are oriented with their plane predominantly parallel to the substrate surface on Au(111) and Ag(111). This effect seems to be more pronounced on the Ag(111) substrate. We omit a quantitative analysis of the average tilt angles since the background affects the normalization of the spectra, in particular in the case of $FePcF_{16}$ on Ag(111). In particular, the slope of the background of the experimental curves at different photon incidence angles and coverages makes the exact determination of the step edge for coverages in the monolayer range complicated. In addition, it is known that weak in-plane transitions appear in the same region as the π^* resonances[30,37,38] because of the hybridization of

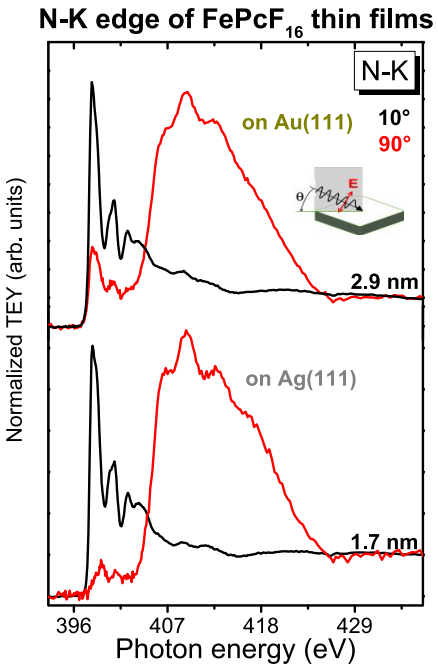

Figure 1. N 1s X-ray absorption spectra of thin films of $FePcF_{16}$ on Au(111) (upper panel) and Ag(111) (lower panel) as a function of the incidence angle θ of the incoming synchrotron light.

unoccupied nitrogen-related states with the d-orbitals of the transition metal atom.[39−42]

3.2. Interface Properties of the Macrocycle of $FePcF_{16}$ on Au(111) and Ag(111). Between phthalocyanines and a multitude of substrates, different interaction channels were observed, involving both the macrocycle and the central metal atom. In many cases the charge transfer is even bidirectional.[13,43−46] First we will discuss the behavior of the macrocycle at interfaces to the less reactive Au(111) and the more reactive Ag(111) substrate.

In Figure 2 we show the thickness-dependent C 1s core-level spectra including detailed peak fits for the bulk-like thin films (thickness ≥ 1.7 nm) and ultrathin films of 1−2 monolayers (ML) coverage. The monolayer (ML) thickness is about 0.32 nm for flat-lying perfluorinated phthalocyanines.[19] At the chosen excitation energy of 385 eV, the recorded C 1s spectra are surface sensitive, and the mean free path of the electrons is about 0.8 nm.[47] The results for $FePcF_{16}$/Au(111) are very similar to recently published data, measured at higher excitation energies.[27]

The spectra recorded at the higher thicknesses of 2.9 and 1.7 nm on Au(111) and Ag(111), respectively, are very similar in their peak shapes. According to the literature, the three main peak components can be assigned to carbon bonded to fluorine (CF), bonded to nitrogen (CN), and bonded to other carbon (CC) atoms, and the respective satellites (S_{CF}, S_{CN}, S_{CC}) from high to low binding energy.[15] The energetic positions of all components are summarized in Table 1. Additional peak fit data are shown in Tables S1 and S2.

For the thin films, the intensity ratios CF/CN/CC of 4.3:1.6:2 and 4.3:1.7:2 for Au(111) and Ag(111), respectively, are in reasonable agreement with the stoichiometry of the differently bound carbon atoms in $FePcF_{16}$ (4:2:2). The intensities of the satellites were added to the intensities of the main components. Small deviations from the expected intensity ratio may be explained by the unknown shape and

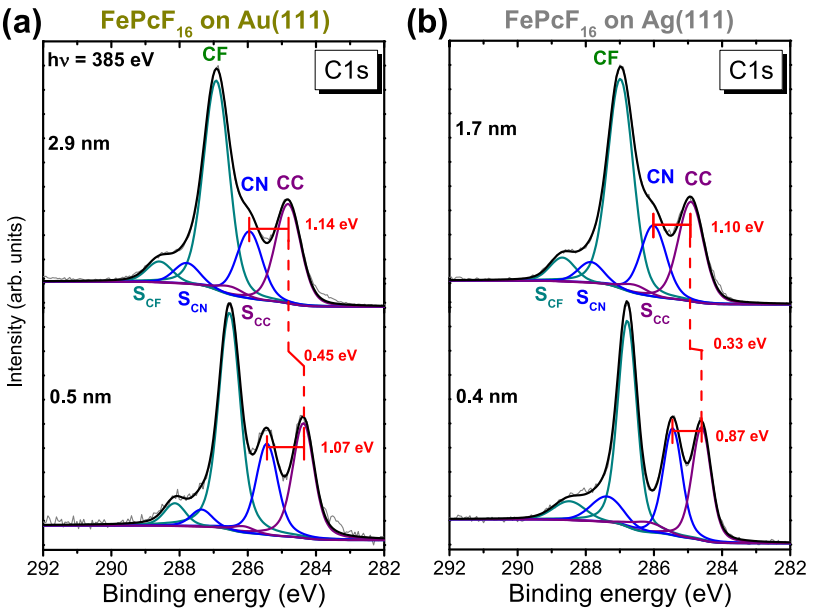

Figure 2. Thickness-dependent C 1s core-level spectra of $FePcF_{16}$ on (a) Au(111) and (b) Ag(111) recorded at an excitation energy of $h\nu$ = 385 eV.

Table 1. $FePcF_{16}$ on Au (111) and Ag(111): Thickness-Dependent C 1s Binding Energies as Obtained from the Peak Fits in eV

substrate	thickness (nm)	CF	S_{CF}	CN	S_{CN}	CC	S_{CC}
Au(111)	2.9	286.92	288.59	285.95	287.79	284.82	286.51
	0.5	286.54	288.14	285.44	287.36	284.37	286.13
Ag(111)	1.7	286.98	288.68	286.01	287.85	284.91	286.57
	0.4	286.79	288.48	286.45	287.38	284.58	286.23

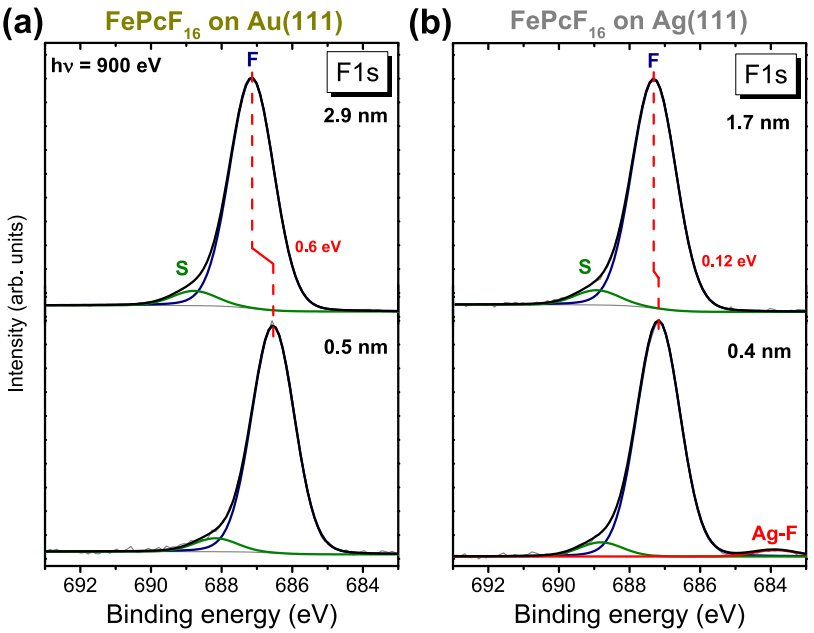

Figure 3. Thickness-dependent F 1s core-level spectra of $FePcF_{16}$ on (a) Au(111) and (b) Ag(111), measured with an excitation energy of $h\nu$ = 900 eV. The additional component in the F 1s monolayer spectrum on Ag(111) may indicate a partial decomposition.

intensity of the satellite features as well as the high surface sensitivity at the chosen excitation energy. It was shown that at high surface sensitivity, the outer carbon atoms appear more intense for almost edge-on oriented phthalocyanines.[48] Considering the (small) tilt angle of the $FePcF_{16}$ molecules on both substrates (cf. Figure 1), the surface-sensitive measurement conditions might result in a higher relative intensity of the outermost carbon (CF) compared to the carbon near the macrocycle center (CN).

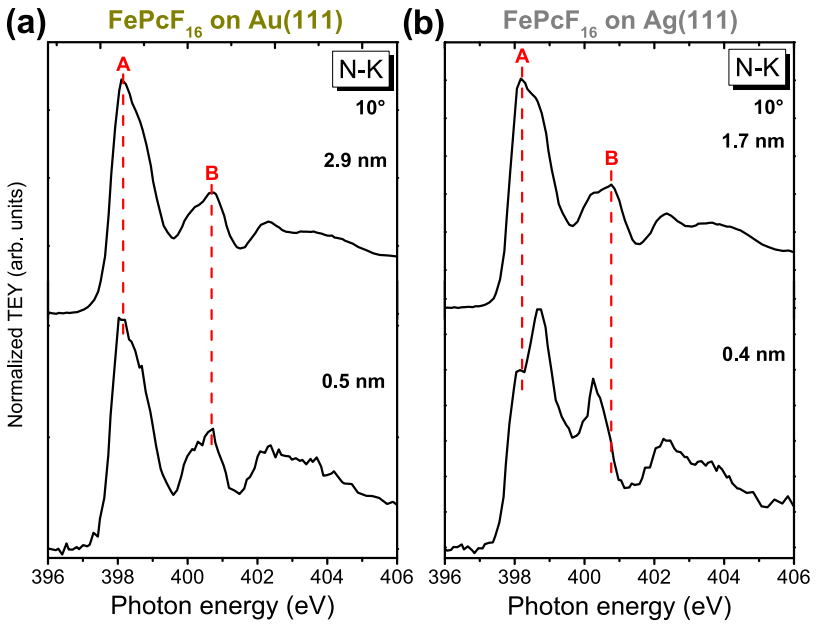

Figure 4. Zoomed-in view of π^* resonances of the N-K edge of $FePcF_{16}$ on (a) Au(111) and (b) Ag(111) as a function of the thickness at grazing incidence (10°). Distinct thickness-dependent changes are observed for $FePcF_{16}$/Ag(111).

The intensity ratio of the components in the C 1s core-level spectrum of the 0.5 nm layer on Au(111) fits rather well to the expected stoichiometry (CF/CN/CC = 4:1.8:2). Larger deviations were observed for the $FePcF_{16}$ monolayer on Ag(111): The intensity ratio of C1s components CF/CN/CC is 3.7:2.3:2. One reason might be the insufficient description of the S_{CF} and S_{CN} satellites (assuming the same shape as the main component) at the interface. Further, a substrate-induced decomposition, as observed for perfluoro-pentacene on Cu (111) after annealing,[49] cannot be completely ruled out (see the discussion of the related F 1s spectra below).

The energetic positions of the C 1s components depend on the film thickness. By means of the CC component, the C 1s shifts about 0.45 and 0.33 eV on Au(111) and Ag(111), respectively, to lower binding energies from high to low coverage (Figure 2 and Table 1). Such energetic shifts of the core-level binding energies are expected due to final-state screening effects, which are often in the range of 0.3−0.6 eV.[50−53] The smaller shift on Ag(111) compared to Au(111) may indicate the presence of a different effect (such as interfacial charge transfer or redistribution), which is opposite to the final-state screening effects.

A closer investigation of the relative binding energy shifts of C 1s components reveals distinct differences between the 1−2 ML coverage and thin film. As is clearly visible in Figure 2, the separation between CC and CN is decreased at the interface, most significantly for $FePcF_{16}$/Ag(111). The results for $FePcF_{16}$ are in good agreement with recently published data;[27] smaller differences are ascribed to the slightly different film thicknesses in both cases. On Ag(111), also the CF component is shifted with respect to CC by −0.19 eV for the 1−2 ML coverage compared to the 1.7 nm film (Table 1). Generally, such effects may originate from site-dependent screening and/or a redistribution of charges at the interface.[13,46,54] It seems, however, that the situation is distinctly different for $FePcF_{16}$ on Au (111) and Ag(111).

F 1s core-level spectra for the two coverages of $FePcF_{16}$ on Au(111) and Ag(111) are shown in Figure 3, described by a main component and a related shake-up satellite. The peak fit parameters are summarized in Tables S3−S5 (Supporting Information).

Analogously to C 1s, the lowering of the binding energies of the F 1s core-level spectra in Figure 3 for coverages in the monolayer range can be essentially ascribed to the final-state screening effects in photoemission. Notably, the shift of F 1s is 0.6 eV on Au(111) and just 0.12 eV on Ag(111), whereas N 1s (Figure S1, Tables S3−S5) shifts nearly by the same amounts (0.36 and 0.30 eV on Au(111) and Ag(111), respectively). This may indicate a different participation of the atoms of the macrocycle in the redistribution of charges at the interface, depending on the type of the substrate. On the other hand, also the screening might be different for fluorine atoms at the interface due to a bending of the molecule, as observed for related fluorinated phthalocyanines.[55,56]

A closer inspection of the F 1s spectrum of the 0.4 nm $FePcF_{16}$ coverage on Ag(111) reveals an additional component at 683.9 eV with a relative intensity ratio of 2.5%. The binding energy is in the range of binding energies reported for AgF.[57−59] Therefore, the presence of such an interface peak may indicate the decomposition of some C−F bonds and the formation of new bonds between fluorine and the substrate, similar to AlFPc/Ag,[60] $FePcF_{16}/TiO_2$,[61] or perfluoro-pentacene on Ag and Cu substrates.[62] However, from the low intensity of the interface peak and the peak shape of the C 1s spectrum (Figure 2), we conclude that most C−F bonds are still intact.

Although the thickness-independent peak shapes of the N 1s core-level spectra in Figure S1 (Supporting Information) suggest that N atoms are not involved in the interface interaction on Ag(111), it might be worthwhile to inspect the corresponding N-K edge XAS spectra more in detail (Figure 4). It was reported that especially π^* resonances in the N-K edge absorption spectra are very sensitive to the involvement of nitrogen in the interfacial interactions.[25,61,63,64] A zoomed-in view of the structures at lower photon energies of the already discussed N-K edge XAS spectra (Figure 1) is shown in Figure

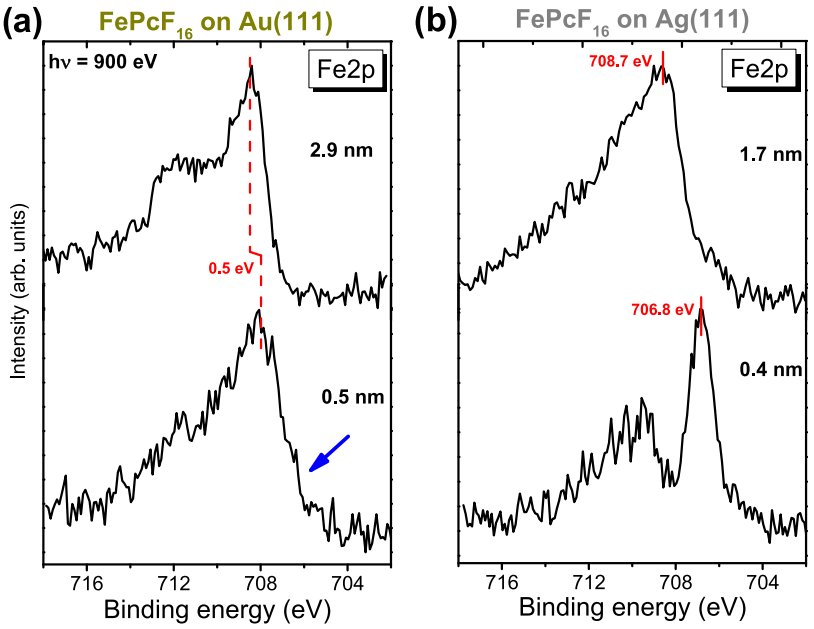

Figure 5. Thickness-dependent Fe2p core-level spectra of $FePcF_{16}$ on (a) Au(111) and (b) Ag(111) measured with an excitation energy of $h\nu$ = 900 eV.

4, for grazing incidence of the incoming synchrotron light (maximal intensity of π^* transitions). The features below 404 eV arise predominantly from transitions into π^* molecular orbitals. For phthalocyanines, most intense π^* resonances (denoted A) are assigned to transitions from N 1s to the lowest unoccupied molecular orbital (LUMO) e_g orbitals.[39,40] The fine structure of feature A arises from an involvement of the ligand LUMO in the hybridization with the central metal atom of the Pc.[13,39,41,42,63,65−67]

There is an obvious difference between the spectra recorded at the different substrate interfaces. While on Au(111) the π^* resonances exhibit very similar spectra for the thin film and 1−2 ML coverage (Figure 4a), they look distinctly different on Ag(111) (Figure 4b). The thin film spectrum on Ag(111) is very similar to the thin film on Au(111) and other thin films of related phthalocyanines.[64] However, the spectra from the 0.4 nm ultrathin film (monolayer range) exhibits striking differences to the former ones. Features A and B decrease drastically. These structures originate from a hybridization between the wave functions of the nitrogen p-orbitals and d-orbitals of the central Fe atom of the phthalocyanine.[13,41,42,63,66,67] A possible reason for the decreased intensities of A and B at the interface to Ag(111) could be the partial filling of the corresponding orbitals, indicating a distinct involvement of the nitrogen atoms in the interaction at the interface.

3.3. Involvement of the Central Iron Atom in the Interaction at the Interface. Besides the macrocycle, also the central metal atom may interact with the substrate. In the case of transition metal phthalocyanines, valuable information about the interactions can help to deliver metal 2p photoemission and excitation spectra. The shapes of both Fe2p XPS and Fe $L_{2,3}$ XAS spectra are largely determined by complex multiplet structures, caused by the overlap of 2p and 3d wave functions.[68] As a consequence, the shapes of these spectra are very sensitive to the d-electronic structure.

Fe2p XPS spectra for the $FePcF_{16}$ multilayer thin films and coverages in the monolayer range on Au(111) and Ag(111) are shown in Figure 5. The multilayer spectra exhibit a broad multiplet structure, typical for iron phthalocyanines (see, e.g., ref 27). Additionally, at the chosen excitation energy, a broad F 1s loss peak appears at a binding energy of about 711 eV; the relative intensity depends, among others, on the detailed molecular orientation and arrangement.

For $FePcF_{16}$ on Au(111), the maximum peak of the spectrum at 0.5 nm coverage (Figure 5a) appears at 0.5 eV lower binding energy compared to the bulk-like thin film, which can be understood analogously to the other core-level spectra, by the final-state screening effects of the photohole. At lower binding energies, an additional shoulder might be visible (the blue arrow in Figure 5a). This points to a non-negligible interaction between the Fe ion of $FePcF_{16}$ and the Au(111) substrate. Such effects were first reported for FePc and related tetrapyrrole monolayers on Au(111)[69,70] and were discussed in more detail for (partially) fluorinated FePc in ref 27. Since the multiplet structure of the Fe2p spectrum of the thin film is almost maintained for the spectrum of the 1−2 ML coverage, it is proposed that only the Fe center of few molecules on particular adsorption sites interacts with the substrate surface.[27]

In contrast, the multiplet structure of the Fe2p XPS spectrum for $FePcF_{16}$ on Ag(111) changes drastically, comparing the multilayer and monolayer spectra in Figure 5b. For 1−2 ML coverages, a new feature at 706.8 eV dominates the spectrum, located at about 2 eV lower binding energy compared to the thin film. This feature can be assigned to the reduced iron, as reported for FePc on Ag(111) or Cu (111).[12,21,25,71]

The corresponding Fe L_3 edge XAS spectra for $FePcF_{16}$ on Au(111) and Ag(111) at grazing and normal incidence of the p-polarized synchrotron light are shown in Figure 6. The angular dependence of the peak shape arises from the selection rules for transitions into different orbitals. For the almost flat-lying molecules (cf. discussion of the angular dependence of the N-K XA spectra, Figure 1), transitions into orbitals with in-plane components (d_{x2-y2} and d_{xy}) are strongest at normal

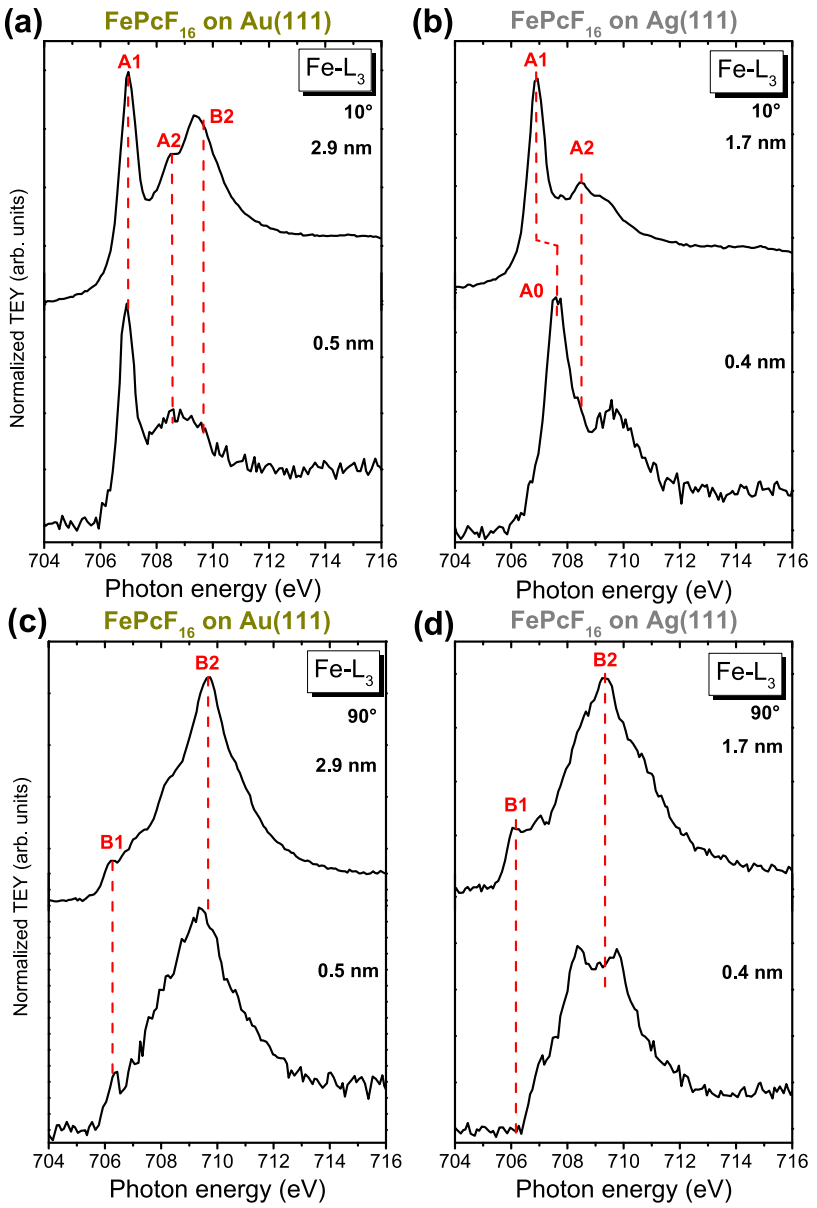

Figure 6. Fe L_3 edge XAS spectra of $FePcF_{16}$ on Au(111) (a, c) and Ag(111) (b, d) as a function of the thickness at grazing and normal incidence. The feature A0 at grazing incidence for $FePcF_{16}$/Ag(111) (b) can be understood by a hybridization of Fe and substrate-related orbitals at the interface.

incidence, while at grazing incidence, transitions into orbitals with out-of-plane components (d_{xz}, d_{yz}, d_{z2}) are most intense. For a detailed discussion of the spectral shape of Fe L edge XAS spectra, we refer to the literature (e.g., refs 11, 41, 42). In Figure 6, the prominent features in the spectra recorded at grazing incidence are labeled "A" and represent out-of-plane transitions (into orbitals with out-of-plane components, such as a_{1g} and e_g), while the features labeled "B" observed at normal incidence conditions represent in-plane transitions, dominated by excitations into b_{1g} and b_{2g} orbitals.

The multilayer Fe-L_3 edge spectra on both substrates shown in Figure 6 exhibit the typical features observed for predominantly flat-lying FePc or $FePcF_{16}$ molecules.[25,72] Features A1 and B2 clearly dominate the spectra at grazing and normal incidence, respectively. We note that also different, broader spectral shapes were observed for flat-lying $FePcF_{16}$ molecules, in particular at grazing incidence.[12] Such effects might be attributed to the influence of the detailed arrangement and packing on the spin state of the iron ion.[12] Also, the Fe-L_3 edge spectra of the thin $FePcF_{16}$ film on Au(111) exhibit in Figure 6a a somewhat untypical low relative intensity of A1 and an additional stronger peak at photon energies only 0.3 eV lower than B2. However, most likely, these differences can be ascribed to the increased tilt angle of the molecules with respect to the substrate surface in thicker films on Au(111) (cf. Figure 1) compared to the monolayer. The corresponding angle-dependent N-K edge spectra for monolayer coverages are shown in Figure S2 (Supporting Information). As a consequence, the features in the Fe L_3 XAS spectra of thicker films arising from in-plane transitions are enhanced at grazing incidence.

Most importantly, whereas only minor thickness-dependent changes of the spectral shape can be identified for $FePcF_{16}$ on Au(111) in Figure 6, clear differences are visible on the

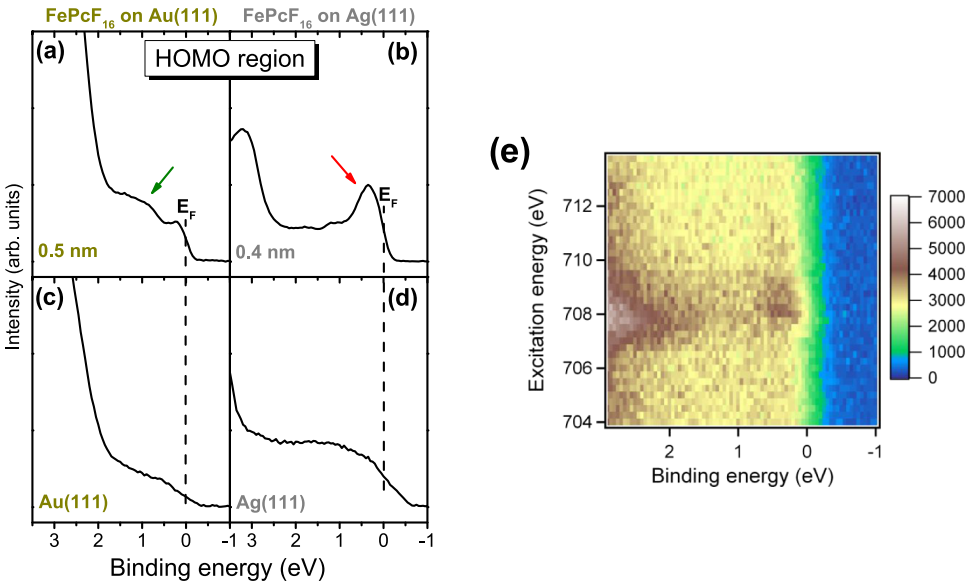

Figure 7. Zoomed-in view of the HOMO region of (a) 0.5 nm $FePcF_{16}$ on Au(111) and (b) 0.4 nm on Ag(111) compared to the clean substrates (c, d). The excitation energy for (a–d) is $h\nu$ = 140 eV (normal emission). (e) Intensity plot of the valence band spectra for excitation energies in the range of the Fe L_3 absorption edge (resonant photoemission spectroscopy, ResPES) for 0.4 nm $FePcF_{16}$ on Ag(111). For excitation, a linearly polarized light with an angle of incidence of $\theta = 40°$ was used. The intensity enhancement at about 708 eV reveals the Fe character of the interface state.

Ag(111) substrate. For 1–2 ML coverages on Ag(111), a new feature, A0, dominates the spectrum at grazing incidence (at 0.8 eV lower photon energy compared to A1), while A1 disappears completely. Analogously to related systems,[13,64] feature A0 can be understood by a hybridization of Fe-related and substrate-related orbitals as a result of the chemisorption of $FePcF_{16}$ on the substrate surface. At normal incidence (Figure 6d), feature B1 disappears for low coverages and the shape of the features at higher photon energies changes, indicating a filling and redistribution of d-electrons. This demonstrates that the d-orbitals related to feature A1 at grazing incidence and features B1 and B2 at normal incidence are involved in the interaction between the central metal Fe atom of $FePcF_{16}$ and Ag(111). These features result from transitions into all 3d-orbitals, except the $3d_{xy}$-orbital (e.g., refs 11, 41, 42). We note that simulations of such spectra, as reported for $FePcF_{16}$ thin films,[11,12] are beyond the scope of this study. Besides a unidirectional charge transfer, most likely mixed valences and strong correlation effects have to be considered, as demonstrated for CoPc and FePc on Au(111).[73]

In order to shed more light on the different interactions of $FePcF_{16}$ on both substrates, we analyze the corresponding valence band spectra in more detail (Figure 7). The interactions at the interfaces may result in the formation of new states in the band gap and/or in the appearance of former unoccupied states in the occupied electronic structure. At the chosen photon energy of 140 eV (Figure 7a–d), the relative intensity of states with Fe character is enhanced according to the corresponding photoelectron cross sections.[28]

The spectra for 1–2 monolayer coverages in Figure 7a,b are compared to those of the clean substrate (Figure 7c,d). On both clean substrates, no features in the highest occupied molecular orbital (HOMO) region can be detected and thus, all features in the 1–2 ML spectra can be assigned to $FePcF_{16}$. In the spectra representing 1–2 ML coverage, distinct substrate-dependent differences are visible. On Au(111), a comparable broad feature appears (green arrow in Figure 7a), which can be assigned to the interface HOMO of $FePcF_{16}$ with a typical binding energy of about 1 eV.[72] In contrast, on Ag(111), a sharp feature appears at a binding energy of 0.4 eV, shown by the red arrow in Figure 7b. This feature can be assigned to the formation of an interface state: for example, caused by a partial filling of the LUMO of the molecules as a consequence of the charge transfer,[46,74] or a formation of new states caused by hybridization between Fe d-orbitals and substrate-related states, as proposed for related $CoPcF_{16}$/metal interfaces.[46,75,76] We note that such an interface state is often observed for strongly interacting metal phthalocyanine/metal systems, including FePc on Ag(111).[25]

The question may arise if the interface state originates from the interaction of the macrocycle or the Fe ion of $FePcF_{16}$ with the Ag(111) substrate. For the analysis of the contribution of different chemical species to particular valence band features, Resonant photoemission spectroscopy (ResPES) can be utilized (see, e.g., ref 77). After a resonant excitation of an electron into unoccupied molecular levels (i.e., at the photon energies of the XAS resonances), different possible non-radiative de-excitation channels of the resulting core hole cause substantial changes in spectral valence band features: normal Auger electron emission, participator decay (ResPES), and spectator decay (resonant Auger spectroscopy).[77]

In order to probe a possible contribution of Fe to the interface peak, we performed ResPES at excitation energies in the range of the Fe L_3 edge for $FePcF_{16}$ (0.4 nm) on Ag(111). The intensity plot in Figure 7e shows a distinct intensity enhancement for binding energies between 0 and 2 eV and an excitation energy of about 708 eV (photon energy of the A0 resonance, cf. Figure 6b). The additional intensity, most notably right above the Fermi edge at around 0.4 eV, is caused by resonant excitation from the Fe2p core level, similar to FePc on Ag(111).[25] The data clearly show that the gap states (interface states) at the Fermi edge possess a distinct iron character and thus, these findings provide an additional hint for a strong interaction of the central metal atom on the interface

to Ag(111). From Fe2p excitation and photoemission spectra, a hybridization of Fe d-orbitals (most likely d_{z2}) with substrate-related orbitals associated with a charge transfer to the Fe ion was already proposed (Figures 5 and 6). Therefore, the additional intensity in Figure 7d might be attributed to a large extent to a filled Fe d-orbital at the interface to Ag(111).

4. CONCLUSIONS

We studied the electronic structure and orientation of thin films a nd 1 −2 M L c ov erageo f F ePcF$_{16}$ o n A g(111) and compared the data to FePcF$_{16}$ on Au(111). On both the studied substrates, FePcF$_{16}$ grows in a preferred flat-lying adsorption geometry. The average molecular tilts are larger on the Au(111) surface. While the interaction between FePcF$_{16}$ and Au(111) is comparably weak, we report a strong interaction between FePcF$_{16}$ and Ag(111), inv olv ingboth the FePcF$_{16}$ macrocycle and the central Fe atom. XPS core-lev el shifts and changes in the N-K edge absorption spectra indicate charge transfer from the Ag(111) substrate to the macrocycle. Thickness-dependent Fe2p core-level and $L_{3,2}$ edge absorption spectra rev eal that the electronic structure of the central Fe atom is distinctly changed at the Ag(111) interface. As a consequence of this strong interaction, an interface state occurs close to the Fermi energy, which exhibits considerable Fe character.

A comparison of FePcF$_{16}$/Ag(111) to the previously inv estigated FePc/Ag(111)[25] interfaces rev eals that in both cases a charge transfer from the substrate to the central Fe ion occurs and interface-related v alence band features with Fe character may be identified. Thus, in these cases of strong and local interactions, the substantial tuning of the ionization potential by fluorination of the molecule has apparently only a minor influence o n t he s trength a nd n ature o f i nteractions at the interfaces.

AUTHOR INFORMATION

Corresponding Author

Heiko Peisert − *Institute of Physical and Theoretical Chemistry, University of Tübingen, 72076 Tübingen, Germany;* orcid.org/0000-0002-9742-5800; Phone: (+49) 07071/29-76931; Email: heiko.peisert@uni-tuebingen.de; Fax: (+49) 07071 / 29-5490

Authors

Axel Belser − *Institute of Physical and Theoretical Chemistry, University of Tübingen, 72076 Tübingen, Germany*

Katharina Greulich − *Institute of Physical and Theoretical Chemistry, University of Tübingen, 72076 Tübingen, Germany*

Peter Nagel − *Karlsruher Institut für Technologie, Institut für Quantenmaterialien und -Technologien (IQMT), 76021 Karlsruhe, Germany; Karlsruhe Nano Micro Facility (KNMFi), Karlsruhe Institute of Technology (KIT), 76344 Eggenstein-Leopoldshafen, Germany*

Michael Merz − *Karlsruher Institut für Technologie, Institut für Quantenmaterialien und -Technologien (IQMT), 76021 Karlsruhe, Germany; Karlsruhe Nano Micro Facility (KNMFi), Karlsruhe Institute of Technology (KIT), 76344 Eggenstein-Leopoldshafen, Germany;* orcid.org/0000-0002-7346-7176

Stefan Schuppler − *Karlsruher Institut für Technologie, Institut für Quantenmaterialien und -Technologien (IQMT), 76021 Karlsruhe, Germany; Karlsruhe Nano Micro Facility (KNMFi), Karlsruhe Institute of Technology (KIT), 76344 Eggenstein-Leopoldshafen, Germany*

Thomas Chassé − *Institute of Physical and Theoretical Chemistry, University of Tübingen, 72076 Tübingen, Germany; Center for Light-Matter Interaction, Sensors & Analytics (LISA$^+$) at the University of Tübingen, 72076 Tübingen, Germany;* orcid.org/0000-0001-6442-8944

Notes

The authors declare no competing financial interest.

ACKNOWLEDGMENTS

The authors are grateful to the Synchrotron Light Source KARA (Karlsruhe, Germany) for the provision of beamtime.

REFERENCES

(1) Urbani, M.; Ragoussi, M.-E.; Nazeeruddin, M. K.; Torres, T. Phthalocyanines for Dye-Sensitized Solar Cells. *Coord. Chem. Rev.* **2019**, *381*, 1−64.

(2) Boileau, N. T.; Cranston, R.; Mirka, B.; Melville, O. A.; Lessard, B. H. Metal Phthalocyanine Organic Thin-Film Transistors: Changes in Electrical Performance and Stability in Response to Temperature and Environment. *RSC Adv.* **2019**, *9*, 21478−21485.

(3) Wang, X. W.; Xiao, C. C.; Yang, C.; Chen, M. G.; Yang, S. Y. A.; Hu, J.; Ren, Z. H.; Pan, H.; Zhu, W. U.; Xu, Z. A.; Lu, Y. Ferroelectric Control of Single-Molecule Magnetism in 2D Limit. *Sci. Bull.* **2020**, *65*, 1252−1259.

(4) Schmidt, A. M.; Calvete, M. J. F. Phthalocyanines: An Old Dog Can Still Have New (Photo)Tricks! *Molecules* **2021**, *26*, No. 2823.

(5) Liu, J. H.; Luo, K.; Chang, H. D.; Sun, B.; Wu, Z. H. Ultrahigh Spin Filter Efficiency, Giant Magnetoresistance and Large Spin Seebeck Coefficient in Monolayer and Bilayer Co-/Fe-/Cu-Phthalocyanine Molecular Devices. *Nanomaterials* **2021**, *11*, No. 2713.

(6) Song, Y.; Wang, C. K.; Chen, G.; Zhang, G. P. A First-Principles Study of Phthalocyanine-Based Multifunctional Spintronic Molecular Devices. *Phys. Chem. Chem. Phys.* **2021**, *23*, 18760−18769.

(7) Tong, J. W.; Luo, F. F.; Ruan, L. X.; Liu, G. H.; Zhou, L. Q.; Tian, F. B.; Qin, G. W.; Zhang, X. M. Interfacial Antiferromagnetic Coupling and High Spin Polarization in Metallic Phthalocyanines. *Phys. Rev. B* **2021**, *103*, No. 024435.

(8) Miedema, P. S.; Stepanow, S.; Gambardella, P.; de Groot, F. M. F. 2p X-Ray Absorption of Iron-Phthalocyanine, 14th International Conference on X-Ray Absorption Fine Structure, DiCicco, A.; Filipponi, A., Eds.; Iop Publishing Ltd: Bristol, 2009; Vol. *190*.

(9) Miedema, P. S.; de Groot, F. M. F. The Iron L Edges: Fe 2p X-Ray Absorption and Electron Energy Loss Spectroscopy. *J. Electron Spectrosc. Relat. Phenom.* **2013**, *187*, 32−48.

(10) Kuz'min, M. D.; Savoyant, A.; Hayn, R. Ligand Field Parameters and the Ground State of Fe(II) Phthalocyanine. *J. Chem. Phys.* **2013**, *138*, No. 244308.
(11) Greulich, K.; Trautmann, M.; Belser, A.; Bolke, S.; Karstens, R.; Nagel, P.; Schuppler, S.; Merz, M.; Chassé, A.; Chassé, T.; Peisert, H. Influence of the Fluorination of Iron Phthalocyanine on the Electronic Structure of the Central Metal Atom. *J. Phys. Chem. C* **2021**, *125*, 6851−6861.
(12) Belser, A.; Karstens, R.; Grüninger, P.; Nagel, P.; Merz, M.; Schuppler, S.; Suturina, E. A.; Chassé, A.; Chassé, T.; Peisert, H. Spin State in Perfluorinated FePc Films on Cu(111) and Ag(111) in Dependence on Film Thickness. *J. Phys. Chem. C* **2018**, *122*, 15390−15394.
(13) Belser, A.; Karstens, R.; Nagel, P.; Merz, M.; Schuppler, S.; Chassé, T.; Peisert, H. Interaction Channels between Perfluorinated Iron Phthalocyanine and Cu(111). *Phys. Status Solidi* **2019**, *256*, No. 1800292.
(14) Peisert, H.; Knupfer, M.; Fink, J. Electronic Structure of Partially Fluorinated Copper Phthalocyanine (Cupcf4) and Its Interface to Au(100). *Surf. Sci.* **2002**, *515*, 491−498.
(15) Peisert, H.; Knupfer, M.; Schwieger, T.; Fuentes, G. G.; Olligs, D.; Fink, J.; Schmidt, T. Fluorination of Copper Phthalocyanines: Electronic Structure and Interface Properties. *J. Appl. Phys.* **2003**, *93*, 9683−9692.
(16) Brinkmann, H.; Kelting, C.; Makarov, S.; Tsaryova, O.; Schnurpfeil, G.; Wöhrle, D.; Schlettwein, D. Fluorinated Phthalocyanines as Molecular Semiconductor Thin Films. *Phys. Status Solidi A* **2008**, *205*, 409−420.
(17) Ling, M. M.; Bao, Z. N. Copper Hexafluorophthalocyanine Field-Effect Transistors with Enhanced Mobility by Soft Contact Lamination. *Org. Electron.* **2006**, *7*, 568−575.
(18) Zhang, Y.; Cai, X.; Bian, Y.; Jiang, J. Organic Semiconductors of Phthalocyanine Compounds for Field Effect Transistors (Fets). *Funct. Phthalocyanine Mol. Mater.* **2010**, *135*, 275−321.
(19) Jiang, H.; Ye, J.; Hu, P.; Wei, F.; Du, K.; Wang, N.; Ba, T.; Feng, S.; Kloc, C. Fluorination of Metal Phthalocyanines: Single-Crystal Growth, Efficient N-Channel Organic Field-Effect Transistors and Structure-Property Relationships. *Sci. Rep.* **2015**, *4*, No. 7573.
(20) Yamane, H.; Carlier, A.; Kosugi, N. Orbital-Specific Electronic Interaction in Crystalline Films of Iron Phthalocyanine Grown on Au(111) Probed by Angle-Resolved Photoemission Spectroscopy. *Mater. Chem. Front.* **2018**, *2*, 609−614.
(21) Snezhkova, O.; Bischoff, F.; He, Y. Q.; Wiengarten, A.; Chaudhary, S.; Johansson, N.; Schulte, K.; Knudsen, J.; Barth, J. V.; Seufert, K.; et al. Iron Phthalocyanine on Cu(111): Coverage-Dependent Assembly and Symmetry Breaking, Temperature-Induced Homocoupling, and Modification of the Adsorbate-Surface Interaction by Annealing. *J. Chem. Phys.* **2016**, *144*, No. 094702.
(22) Gargiani, P.; Betti, M. G.; Ibrahimi, A. T.; Le Fevre, P.; Modesti, S. Orbital Symmetry of the Kondo State in Adsorbed FePc Molecules on the Au(110) Metal Surface. *J. Phys. Chem. C* **2016**, *120*, 28527−28532.
(23) Bartolomé, F.; Bunau, O.; Garcia, L. M.; Natoli, C. R.; Piantek, M.; Pascual, J. I.; Schuller, I. K.; Gredig, T.; Wilhelm, F.; Rogalev, A.; Bartolomé, J. Molecular Tilting and Columnar Stacking of Fe Phthalocyanine Thin Films on Au(111). *J. Appl. Phys.* **2015**, *117*, No. 17A735.
(24) Gargiani, P.; Rossi, G.; Biagi, R.; Corradini, V.; Pedio, M.; Fortuna, S.; Calzolari, A.; Fabris, S.; Cezar, J. C.; Brookes, N. B.; Betti, M. G. Spin and Orbital Configuration of Metal Phthalocyanine Chains Assembled on the Au(110) Surface. *Phys. Rev. B* **2013**, *87*, No. 165407.
(25) Petraki, F.; Peisert, H.; Aygül, U.; Latteyer, F.; Uihlein, J.; Vollmer, A.; Chassé, T. Electronic Structure of FePc and Interface Properties on Ag(111) and Au(100). *J. Phys. Chem. C* **2012**, *116*, 11110−11116.
(26) Betti, M. G.; Gargiani, P.; Mariani, C.; Turchini, S.; Zema, N.; Fortuna, S.; Calzolari, A.; Fabris, S. Formation of Hybrid Electronic States in FePc Chains Mediated by the Au(110) Surface. *J. Phys. Chem. C* **2012**, *116*, 8657−8663.
(27) Greulich, K.; Belser, A.; Basova, T.; Chassé, T.; Peisert, H. Interfaces between Different Iron Phthalocyanines and Au(111): Influence of the Fluorination on Structure and Interfacial Interactions. *J. Phys. Chem. C* **2022**, *126*, 716−727.
(28) Yeh, J. J.; Lindau, I. Atomic subshell photoionization cross sections and asymmetry parameters: $1 \leqslant Z \leqslant 103$. *At. Data Nucl. Data Tables* **1985**, *32*, 1−155.
(29) Hesse, R.; Chassé, T.; Streubel, P.; Szargan, R. Error Estimation in Peak-Shape Analysis of XPS Core-Level Spectra Using Unifit 2003: How Significant Are the Results of Peak Fits? *Surf. Interface Anal.* **2004**, *36*, 1373−1383.
(30) Peisert, H.; Biswas, I.; Knupfer, M.; Chassé, T. Orientation and Electronic Properties of Phthalocyanines on Polycrystalline Substrates. *Phys. Status Solidi B* **2009**, *246*, 1529−1545.
(31) Kera, S.; Casu, M. B.; Bauchspiess, K. R.; Batchelor, D.; Schmidt, T.; Umbach, E. Growth Mode and Molecular Orientation of Phthalocyanine Molecules on Metal Single Crystal Substrates: A NEXAFS and XPS Study. *Surf. Sci.* **2006**, *600*, 1077−1084.
(32) Okudaira, K. K.; Setoyama, H.; Yagi, H.; Mase, K.; Kera, S.; Kahn, A.; Ueno, N. Study of Excited States of Fluorinated Copper Phthalocyanine by Inner Shell Excitation. *J. Electron Spectros. Relat. Phenom.* **2004**, *137*−*140*, 137−140.
(33) Forrest, S. R. Ultrathin Organic Films Grown by Organic Molecular Beam Deposition and Related Techniques. *Chem. Rev.* **1997**, *97*, 1793−1896.
(34) Basova, T. V.; Kiselev, V. G.; Dubkov, I. S.; Latteyer, F.; Gromilov, S. A.; Peisert, H.; Chassé, T. Optical Spectroscopy and Xrd Study of Molecular Orientation, Polymorphism, and Phase Transitions in Fluorinated Vanadyl Phthalocyanine Thin Films. *J. Phys. Chem. C* **2013**, *117*, 7097−7106.
(35) Schuster, B. E.; Basova, T. V.; Plyashkevich, V. A.; Peisert, H.; Chassé, T. Effects of Temperature on Structural and Morphological Features of CoPc and CoPcF16 Thin Films. *Thin Solid Films* **2010**, *518*, 7161−7166.
(36) Stöhr, J. *NEXAFS Spectroscopy*; Springer, 1992.
(37) Rocco, M. L. M.; Frank, K. H.; Yannoulis, P.; Koch, E. E. Unoccupied Electronic Structure of Phthalocyanine Films. *J. Chem. Phys.* **1990**, *93*, 6859−6864.
(38) Floreano, L.; Cossaro, A.; Gotter, R.; Verdini, A.; Bavdek, G.; Evangelista, F.; Ruocco, A.; Morgante, A.; Cvetko, D. Periodic Arrays of Cu-Phthalocyanine Chains on Au(110). *J. Phys. Chem. C* **2008**, *112*, 10794−10802.
(39) Willey, T. M.; Bagge-Hansen, M.; Lee, J. R. I.; Call, R.; Landt, L.; van Buuren, T.; Colesniuc, C.; Monton, C.; Valmianski, I.; Schuller, I. K. Electronic Structure Differences between H-2-, Fe-, Co-, and Cu-Phthalocyanine Highly Oriented Thin Films Observed Using NEXAFS Spectroscopy. *J. Chem. Phys.* **2013**, *139*, No. 034701.
(40) Holland, B. N.; Peltekis, N.; Farrelly, T.; Wilks, R. G.; Gavrila, G.; Zahn, D. R. T.; McGuinness, C.; McGovern, I. T. NEXAFS Studies of Copper Phthaloyanine on Ge(001)-2 × 1 and Ge(111)-c(2 × 8) Surfaces. *Phys. Status Solidi* **2009**, *246*, 1546−1551.
(41) Betti, M. G.; Gargiani, P.; Frisenda, R.; Biagi, R.; Cossaro, A.; Verdini, A.; Floreano, L.; Mariani, C. Localized and Dispersive Electronic States at Ordered FePc and CoPc Chains on Au(110). *J. Phys. Chem. C* **2010**, *114*, 21638−21644.
(42) Bartolomé, J.; Bartolomé, F.; Garcia, L. M.; Filoti, G.; Gredig, T.; Colesniuc, C. N.; Schuller, I. K.; Cezar, J. C. Highly Unquenched Orbital Moment in Textured Fe-Phthalocyanine Thin Films. *Phys. Rev. B* **2010**, *81*, No. 195405.
(43) Petraki, F.; Peisert, H.; Uihlein, J.; Aygül, U.; Chassé, T. CoPc and CoPcF16 on Gold: Site-Specific Charge-Transfer Processes. *Beilstein J. Nanotechnol.* **2014**, *5*, 524−531.
(44) Lindner, S.; Treske, U.; Knupfer, M. The Complex Nature of Phthalocyanine/Gold Interfaces. *Appl. Surf. Sci.* **2013**, *267*, 62−65.
(45) Huang, Y.; Wruss, E.; Egger, D.; Kera, S.; Ueno, N.; Saidi, W.; Bucko, T.; Wee, A.; Zojer, E. Understanding the Adsorption of CuPc and ZnPc on Noble Metal Surfaces by Combining Quantum-

Mechanical Modelling and Photoelectron Spectroscopy. *Molecules* **2014**, *19*, 2969−2992.
(46) Belser, A.; Greulich, K.; Grüninger, P.; Karstens, R.; Ovsyannikov, R.; Giangrisostomi, E.; Nagel, P.; Merz, M.; Schuppler, S.; Chassé, T.; Peisert, H. Perfluorinated Phthalocyanines on Cu(110) and Cu(110)-(2 × 1)O: The Special Role of the Central Cobalt Atom. *J. Phys. Chem. C* **2021**, *125*, 8803−8814.
(47) Seah, M. P.; Dench, W. A. Quantitative Electron Spectroscopy of Surfaces: A Standard Data Base for Electron Inelastic Mean Free Paths in Solids. *Surf. Interface Anal.* **1979**, *1*, 2−11.
(48) Biswas, I.; Peisert, H.; Zhang, L.; Chassé, T.; Knupfer, M.; Hanack, M.; Dini, D.; Schmidt, T.; Batchelor, D. Orientation of Differently Substituted Phthalocyanines: First Layers and Thin Films. *Mol. Cryst. Liq. Cryst.* **2006**, *455*, 241−249.
(49) Glowatzki, H.; Heimel, G.; Vollmer, A.; Wong, S. L.; Huang, H.; Chen, W.; Wee, A. T. S.; Rabe, J. P.; Koch, N. Impact of Fluorination on Initial Growth and Stability of Pentacene on Cu(111). *J. Phys. Chem. C* **2012**, *116*, 7726−7734.
(50) Peisert, H.; Knupfer, M.; Fink, J. Energy Level Alignment at Organic/Metal Interfaces: Dipole and Ionization Potential. *Appl. Phys. Lett.* **2002**, *81*, 2400−2402.
(51) Vázquez, H.; Dappe, Y. J.; Ortega, J.; Flores, F. Energy Level Alignment at Metal/Organic Semiconductor Interfaces: "Pillow" Effect, Induced Density of Interface States, and Charge Neutrality Level. *J. Chem. Phys.* **2007**, *126*, No. 144703.
(52) Betti, M. G.; Kanjilal, A.; Mariani, C.; Vázquez, H.; Dappe, Y. J.; Ortega, J.; Flores, F. Barrier Formation at Organic Interfaces in a Cu(100)-Benzenethiolate-Pentacene Heterostructure. *Phys. Rev. Lett.* **2008**, *100*, No. 027601.
(53) Yamane, H.; Yoshimura, D.; Kawabe, E.; Sumii, R.; Kanai, K.; Ouchi, Y.; Ueno, N.; Seki, K. Electronic Structure at Highly Ordered Organic/Metal Interfaces: Pentacene on Cu(110). *Phys. Rev. B* **2007**, *76*, No. 165436.
(54) Peisert, H.; Petershans, A.; Chassé, T. Charge Transfer and Polarization Screening at Organic/Metal Interfaces: Distinguishing between the First Layer and Thin Films. *J. Phys. Chem. C* **2008**, *112*, 5703−5706.
(55) Gerlach, A.; Schreiber, F.; Sellner, S.; Dosch, H.; Vartanyants, I. A.; Cowie, B. C. C.; Lee, T. L.; Zegenhagen, J. Adsorption-Induced Distortion of F16cupc on Cu(111) and Ag(111): An X-Ray Standing Wave Study. *Phys. Rev. B* **2005**, *71*, No. 205425.
(56) Yamane, H.; Gerlach, A.; Duhm, S.; Tanaka, Y.; Hosokai, T.; Mi, Y. Y.; Zegenhagen, J.; Koch, N.; Seki, K.; Schreiber, F. Site-Specific Geometric and Electronic Relaxations at Organic-Metal Interfaces. *Phys. Rev. Lett.* **2010**, *105*, No. 046103.
(57) Gaarenstroom, S. W.; Winograd, N. Initial and Final State Effects in the Esca Spectra of Cadmium and Silver Oxides. *J. Chem. Phys.* **1977**, *67*, 3500−3506.
(58) Kaushik, V. K. XPS Core Level Spectra and Auger Parameters for Some Silver Compounds. *J. Electron Spectrosc. Relat. Phenom.* **1991**, *56*, 273−277.
(59) Wolan, J. T.; Hoflund, G. B. Surface Characterization Study of Agf and Agf2 Powders Using XPS and Iss. *Appl. Surf. Sci.* **1998**, *125*, 251−258.
(60) Polek, M.; Latteyer, F.; Basova, T. V.; Petraki, F.; Aygül, U.; Uihlein, J.; Nagel, P.; Merz, M.; Schuppler, S.; Chassé, T.; Peisert, H. Chemical Reaction of Polar Phthalocyanines on Silver: Chloroaluminum Phthalocyanine and Fluoroaluminum Phthalocyanine. *J. Phys. Chem. C* **2016**, *120*, 24715−24723.
(61) Karstens, R.; Glaser, M.; Belser, A.; Balle, D.; Polek, M.; Ovsyannikov, R.; Giangrisostomi, E.; Chassé, T.; Peisert, H. FePc and FePcF16 on Rutile TiO2(110) and (100): Influence of the Substrate Preparation on the Interaction Strength. *Molecules* **2019**, *24*, 4579.
(62) Schmidt, C.; Breuer, T.; Wippermann, S.; Schmidt, W. G.; Witte, G. Substrate Induced Thermal Decomposition of Perfluoro-Pentacene Thin Films on the Coinage Metals. *J. Phys. Chem. C* **2012**, *116*, 24098−24106.
(63) Petraki, F.; Peisert, H.; Hoffmann, P.; Uihlein, J.; Knupfer, M.; Chassé, T. Modification of the 3d-Electronic Configuration of Manganese Phthalocyanine at the Interface to Gold. *J. Phys. Chem. C* **2012**, *116*, 5121−5127.
(64) Peisert, H.; Uihlein, J.; Petraki, F.; Chassé, T. Charge Transfer between Transition Metal Phthalocyanines and Metal Substrates: The Role of the Transition Metal. *J. Electron Spectrosc. Relat. Phenom.* **2015**, *204*, 49−60.
(65) Kuz'min, M. D.; Hayn, R.; Oison, V. Ab Initio Calculated XANES and XMCD Spectra of Fe(II) Phthalocyanine. *Phys. Rev. B* **2009**, *79*, No. 024413.
(66) Javaid, S.; Bowen, M.; Boukari, S.; Joly, L.; Beaufrand, J. B.; Chen, X.; Dappe, Y. J.; Scheurer, F.; Kappler, J. P.; Arabski, J.; et al. Impact on Interface Spin Polarization of Molecular Bonding to Metallic Surfaces. *Phys. Rev. Lett.* **2010**, *105*, No. 077201.
(67) Åhlund, J.; Nilson, K.; Schiessling, J.; Kjeldgaard, L.; Berner, S.; Mårtensson, N.; Puglia, C.; Brena, B.; Nyberg, M.; Luo, Y. The Electronic Structure of Iron Phthalocyanine Probed by Photoelectron and X-Ray Absorption Spectroscopies and Density Functional Theory Calculations. *J. Chem. Phys.* **2006**, *125*, No. 034709.
(68) Groot, F. d. Multiplet Effects in X-Ray Spectroscopy. *Coord. Chem. Rev.* **2005**, *249*, 31−63.
(69) Schmid, M.; Zirzlmeier, J.; Steinrück, H. P.; Gottfried, J. M. Interfacial Interactions of Iron(II) Tetrapyrrole Complexes on Au(111). *J. Phys. Chem. C* **2011**, *115*, 17028−17035.
(70) Isvoranu, C.; Knudsen, J.; Ataman, E.; Schulte, K.; Wang, B.; Bocquet, M. L.; Andersen, J. N.; Schnadt, J. Adsorption of Ammonia on Multilayer Iron Phthalocyanine. *J. Chem. Phys.* **2011**, *134*, No. 114711.
(71) Bai, Y.; Buchner, F.; Wendahl, M. T.; Kellner, I.; Bayer, A.; Steinrück, H.-P.; Marbach, H.; Gottfried, J. M. Direct Metalation of a Phthalocyanine Monolayer on Ag(111) with Coadsorbed Iron Atoms. *J. Phys. Chem. C* **2008**, *112*, 6087−6092.
(72) Greulich, K.; Belser, A.; Bölke, S.; Grüninger, P.; Karstens, R.; Sättele, M. S.; Ovsyannikov, R.; Giangrisostomi, E.; Basova, T. V.; Klyamer, D. D.; et al. Charge Transfer from Organic Molecules to Molybdenum Disulfide: Influence of the Fluorination of Iron Phthalocyanine. *J. Phys. Chem. C* **2020**, *124*, 16990−16999.
(73) Stepanow, S.; Miedema, P. S.; Mugarza, A.; Ceballos, G.; Moras, P.; Cezar, J. C.; Carbone, C.; de Groot, F. M. F.; Gambardella, P. Mixed-Valence Behavior and Strong Correlation Effects of Metal Phthalocyanines Adsorbed on Metals. *Phys. Rev. B* **2011**, *83*, No. 220401.
(74) Schwieger, T.; Peisert, H.; Knupfer, M. Direct Observation of Interfacial Charge Transfer from Silver to Organic Semiconductors. *Chem. Phys. Lett.* **2004**, *384*, 197−202.
(75) Rückerl, F.; Waas, D.; Büchner, B.; Knupfer, M. Particular Electronic Properties of F16CoPc: A Decent Electron Acceptor Material. *J. Electron Spectrosc. Relat. Phenom.* **2017**, *215*, 1−7.
(76) Lindner, S.; Treske, U.; Grobosch, M.; Knupfer, M. Charge Transfer at F16CoPc and CoPc Interfaces to Au. *Appl. Phys. A* **2011**, *105*, 921−925.
(77) Brühwiler, P. A.; Karis, O.; Mårtensson, N. Charge-Transfer Dynamics Studied Using Resonant Core Spectroscopies. *Rev. Mod. Phys.* **2002**, *74*, 703−740.